Coordination and Haptotropic Rearrangement of $Cr(CO)_3$ on (*n*,0) Nanotube Sidewalls: A Dynamical Density Functional Study

Francesca Nunzi,[†] Francesco Mercuri,[‡] Filippo De Angelis,[‡] Antonio Sgamellotti,*[,†,‡] Nazzareno Re,[§] and Paolo Giannozzi[||]

Dipartimento di Chimica, Università di Perugia, Via Elce di Sotto 8, I-06123 Perugia, Italy, Istituto CNR di Scienze e Tecnologie Molecolari (ISTM), c/o Dipartimento di Chimica, Università di Perugia, Via Elce di Sotto 8, I-06123 Perugia, Italy, Facoltà di Farmacia, Università G. D'Annunzio, I-66100 Chieti, Italy, and NEST-INFM, Scuola Normale Superiore di Pisa, Piazza dei Cavalieri 7, I-56126 Pisa, Italy

Received: December 4, 2003; In Final Form: February 11, 2004

Static and dynamical density functional theory calculations have been carried out to investigate the coordination and haptotropic rearrangement of the $Cr(CO)_3$ fragment on the (6,0) carbon nanotube sidewalls. Geometry optimizations have been performed on the $Cr(CO)_3-(C_{72}H_{12})$ complex, pointing out the preferred coordination sites of the metal fragment on the nanotube sidewalls. We find a hole site configuration of the $Cr(CO)_3$ to be the global energy minimum of the $Cr(CO)_3-(C_{72}H_{12})$ system, with a binding energy of 143 kJ mol^{-1}. The shifting of the $Cr(CO)_3$ complex between two coordination sites on adjacent hexagonal rings of (6,0) carbon nanotubes has been investigated by means of Car−Parrinello simulations, from which the transition state structure for the haptrotropic rearrangement has been localized and found to be 68 kJ mol^{-1} above the global minimum structure.

1. Introduction

One of the most attractive goals of the scientific community is nowadays the investigation of nanotechnology applications,[1] i.e. the design and manufacture of electronic circuits and mechanical devices employing particles (atoms and molecules) smaller than 100 nm. A great boost to the research on nanotechnology has been provided by the discovery of carbon nanotubes (CNTs) by Ijima in 1991.[2] The unique microscopic structure of CNTs and their remarkable electronic properties make them ideal candidates for use in fuel cells (batteries), electron devices (semiconductors), catalysts, and STM probes.[3] Although several potential applications have been envisaged, chemical modification will be conclusive to foster practical applications of CNTs.[4] Banerjee and Wong opened the field of the organometallic chemistry of CNTs, by functionalizing the tubes with Vaska's complex[5] and then with Wilkinson's catalyst.[6] They showed that the covalent functionalization with transition metals complexes makes CNTs soluble and stable in organic solution, allowing their further manipulation and their use in homogeneous catalysis. Most notably, the covalent attachment of appropriate moieties to CNTs sidewalls provides the means of tuning the electronic and mechanical properties of the tubes in a controllable manner.[7] Even though the limited number of reactions investigated up to date proves that chemical modification of CNTs is still a challenging task, the latest developments in several laboratories highlight a promising growth of the CNTs chemistry.[8] Interestingly, the synthesis of a CNT adduct with $Cr(CO)_3$ was recently attempted by Wilson; however, experimental difficulties in the manipulation of CNTs made ineffective the characterization of the final reaction product.[9]

Theoretical investigations can be very helpful toward a comprehensive understanding of the various factors controlling the chemistry of CNTs.[10] Although several studies have been performed on the chemical functionalization of CNTs sidewalls,[11] only a few works have been carried out employing DFT methods on the interaction of CNTs with transition metals complexes,[12,13] and more detailed investigations are quickly needed. In this paper, we focus on the investigation of $Cr(CO)_3$ coordination on the (6,0) CNT sidewalls by means of both static and dynamical density functional theory (DFT) calculations. The coordination of $Cr(CO)_3$ with polycyclic aromatic hydrocarbons, composed of six member rings topologically resembling the honeycomb lattice of CNTs, has attracted great interest in the past both experimentally and theoretically.[14] These organic substrates can be regarded as precursor building blocks of CNTs and may suggest some interesting hints on the functionalization of the tubes, since both theoretical and experimental studies show that the structure and reactivity of arenes are significantly altered upon complexation with $Cr(CO)_3$ complex.[15] Moreover, since complexed arenes are characterized by high lability, dynamical processes may arise at some temperature, in which the transition metal unit migrates from one coordination site to another in the organic substrate.[16] These rearrangements of the $Cr(CO)_3$ complex, known as haptotropic rearrangements,[17] were first investigated at the extended Hückel level by Albright and Hoffmann in 1983,[16a] who reported the mechanistic features and the minimum energy pathway for $Cr(CO)_3$ rearrangement on bicyclic polyenes. Since the honeycomb lattice of CNTs resembles the hexagonal rings pattern of polycyclic hydrocarbons, it is very interesting to analyze the haptotropic rearrangement of the $Cr(CO)_3$ complex on the CNTs sidewalls, with the aim of localizing the preferred coordination sites and to gain

* Corresponding author. E-mail: sgam@thch.unipg.it. Telephone: +39 075 5855516. Fax: +39 075 5855606.
[†] Dipartimento di Chimica, Università di Perugia.
[‡] Istituto CNR di Scienze e Tecnologie Molecolari (ISTM), c/o Dipartimento di Chimica, Università di Perugia.
[§] Università G. D'Annunzio.
[||] Scuola Normale Superiore di Pisa.

10.1021/jp037705i CCC: $27.50
Published on Web 04/03/2004

insight into the mechanism of the chromium shifting on the hexagonal rings.

In the following, we report gradient corrected DFT calculations on the coordination and haptotropic rearrangement of $Cr(CO)_3$ on the (6,0) CNT sidewalls, using suitable molecular models to describe the local interaction of the metal complex on the (6,0) CNT sidewalls. Moreover, ab initio molecular dynamics simulations (AIMD), by means of the Car−Parrinello (CP) method,[18] have been carried out to characterize the dynamics of the haptotropic rearrangement of $Cr(CO)_3$ on the CNT sidewalls.

2. Computational Details

2.1. Static DFT Calculations. The "static" DFT calculations reported in this paper have been performed by the Amsterdam density functional (ADF) program package.[19] Full geometry optimizations were carried out using the local density approximation of Vosko, Wilk, and Nusair (LDA VWN),[20] augmented with the gradient corrections of Becke[21] and Perdew[22] for exchange and correlation, respectively. The molecular orbitals were expanded in an uncontracted double-ζ Slater-type orbital (STO) basis set for all atoms, with the exception of the chromium orbitals for which a double-ζ STO basis set is used for 3s and 3p and a triple-ζ STO basis set for 3d and 4s. The frozen core is constituted by 1s−3p for Cr, 1s for O and C. One polarization function is added for Cr(4p), for C and O(3d) and for H(2p).

Using the decomposition energy scheme proposed by Ziegler,[23] the binding energy (BE) between the organic moiety and the metal fragment has been partitioned into deformation energy (DE) and steric (E_{ster}) and orbital (E_{orb}) contributions. The basis set superposition error (BSSE) is calculated by applying the counterpoise method.[24] Good agreement between calculated parameters and available experimental data was found in previous calculations on the coordination of transition metal complexes with carbon systems.[12,25]

2.2. Car—Parrinello Calculations. Ab initio molecular dynamics simulations were carried out with the Car−Parrinello (CP) method;[18] all the calculations reported here have been performed with the parallel version[26] of the CP code[27,28] implementing Vanderbilt pseudo-potentials.[28] For the LDA exchange-correlation functional the Perdew−Zunger parametrization[29] has been used, while the gradient-corrected functional is taken from ref 30. Core states are projected out using pseudopotentials. For Cr, C, O, and H, "ultra-soft" pseudopotentials were generated according to the scheme proposed by Vanderbilt.[29] The wave functions were expanded in plane waves up to an energy cutoff of 25 and 240 Ry for the wave functions and density, respectively. Periodic boundary conditions were used by placing the model molecule in a box of sides 12.78 × 15.87 × 15.87 Å, keeping a minimum of 6.0 Å between repeated images along the directions transversal to the CNT axis, aligned along the *x* axis, sufficiently large to avoid any coupling between periodic replicas. The equations of motion were integrated using a time step of 10.0 au (0.242 fs) with an electronic fictitious mass $\mu = 1000$ au. The consistency of the ADF and CP programs has been already demonstrated for several organometallic systems,[31] and it is checked in the present case; see below.

All the calculations have been performed on the IBM-SP Power3 computer at ISTM, Perugia, Italy. A typical ADF single point energy and energy gradients evaluation require ca. 12 CPU hours (ca. 6 h for each step) on a single processor, while a CP integration time step requires ca. 1 CPU minute when run in parallel on eight processors.

SCHEME 1

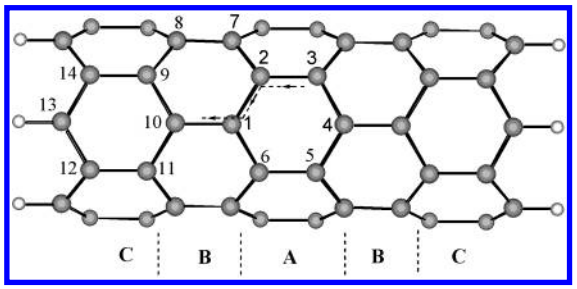

3. Results and Discussion

An adequate description of the interaction between transition metal complexes and CNT sidewalls requires a suitable modeling of the organic moiety. Tubes of finite length modeling (6,0) CNT have been used to examine the coordination of the $Cr(CO)_3$ complex on the sidewalls of (*n*,0) CNTs. The interaction of the metal fragment on the CNT sidewalls has been investigated by considering an η^6, η^2, and η^1 bond fashion of the chromium atom on the six-member rings. Indeed, the η^6 bond fashion has revealed to be the favored one for the coordination of $Cr(CO)_3$ both with benzene[14−16] and with polycyclic aromatic hydrocarbons.[12b] According to previous studies, smaller diameters tubes exhibit greater reactivity, due to the increased curvature of carbon atoms surface.[32] Modeling (6,0) CNTs, with a diameter close to 0.5 nm, allows us to highlight the differences between the coordination chemistry of curved carbon surfaces with respect to planar systems, such as graphene. Furthermore, since functionalized CNTs are still computationally demanding systems, narrower tubes allows us to increase the length of the tube model, while limiting the number of carbon atoms, i.e., the number of basis functions of the overall computation, and keeping a consistent length/diameter ratio.

A (6,0) tube model constituted by five hexagonal rings belts has been considered, where the terminal dangling bonds are saturated with hydrogen atoms ($C_{72}H_{12}$). Hereafter we will consider the labels for the carbon atoms and for the hexagonal belts reported in Scheme 1. A geometry optimization has been performed on this system, imposing D_{6h} symmetry constraints. The calculated C−C bond values compare well with experimental values for CNTs (1.44 Å);[33] in particular, the C−C bond distances on the middle belt **A** show values equal to 1.438 and 1.414 Å for C1−C2 and C2−C3, respectively. Also, calculated C−C values on the boundary belt **C** (1.429 and 1.421 Å for C11−C12 and C12−C13, respectively) show only slight differences from those calculated for the middle belt **A** and the two adjacent ones, **B** (1.416 and 1.436 Å for C1−C10 and C9−C10, respectively), which in turn show essentially the same C−C values. (*n*,0) zigzag CNTs with *n* being a multiple of 3 are expected to be metallic systems.[33] Accordingly, a HOMO−LUMO gap of only 29 kJ mol^{-1} (0.3 eV) has been found for the (6,0)-$C_{72}H_{12}$ tube model in its ground state, the finite value of the HOMO−LUMO gap being due to the finite size of the model system.

Geometry optimizations have then been performed on the $Cr(CO)_3$−($C_{72}H_{12}$) complex, setting the metal fragment on one of the hexagonal rings of the middle belt **A** (see Scheme 1), which is expected to reproduce, with a good degree of approximation, the local metal−ligand interaction of infinite CNT sidewalls. To investigate the potential energy surface of this adduct, we first performed constrained geometry optimiza-

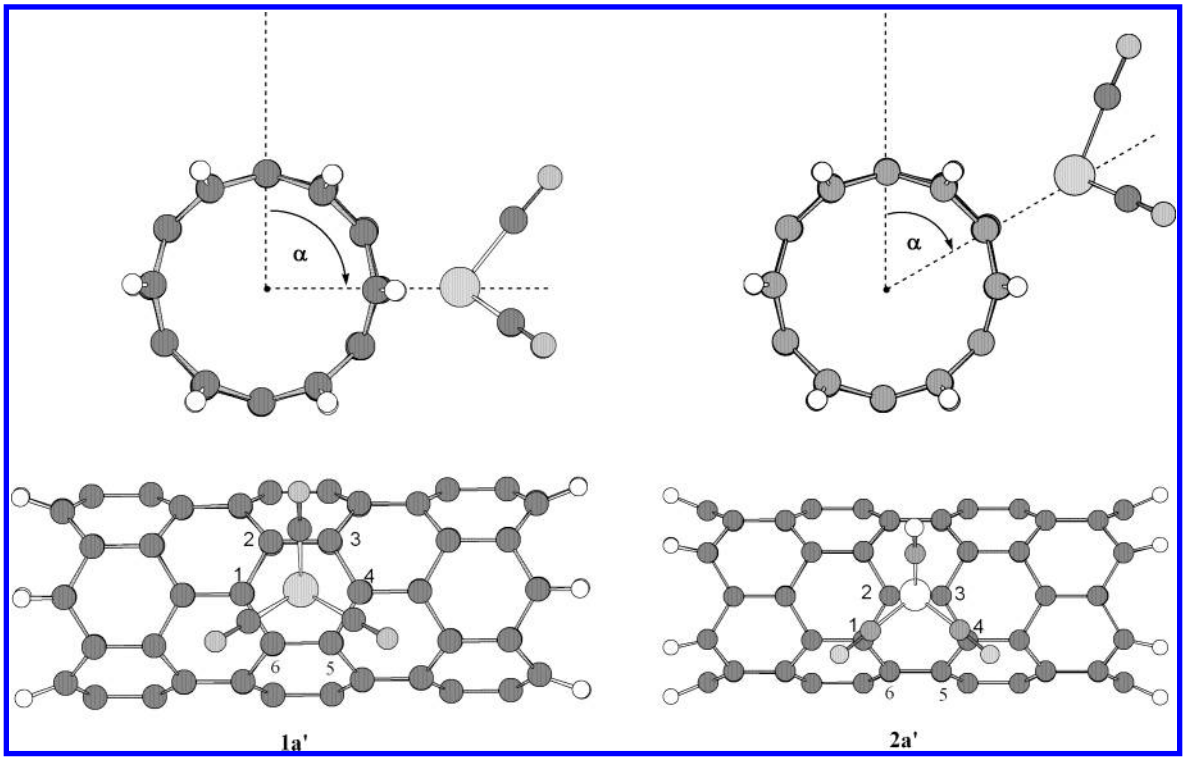

Figure 1. Optimized $Cr(CO)_3-(C_{72}H_{12})$ structures, obtained constraining the parameter α, defined as the angle formed by the Cr atom, the center of the tube and the plane containing the C2−C3 bond, at values of 90°, **1a′** structure, and 60°, **2a′** structure.

tions under C_s symmetry, fixing the angle α, defined as the angle formed by the Cr atom, the center of the tube and the plane containing the C2−C3 bond, at values of 90 and 60° (see Figure 1). According to Figure 1, the **1a′** structure, with α = 90°, corresponds to an η^6 coordination where the chromium atom lies in the middle of the hexagon, while **2a′** structure, with α = 60°, corresponds to an η^2 coordination where the chromium atom lies above the C5−C6 bond. Starting from the optimized structures with α = 90° and α = 60°, full geometry optimizations have then been performed under C_s symmetry. The global minimum of the $Cr(CO)_3$-(6,0) system is represented by a hole site configuration, **1a** in Figure 2, where the metal fragment is in a staggered orientation with respect to the underlying C−C bonds. A binding energy (BE) of 143 kJ mol^{-1} has been calculated for complex **1a**, which is characterized by an α value of 83° and results 16 kJ mol^{-1} lower in energy with respect to the constrained optimized adduct **1a′**, with α = 90°. The corresponding conformer of **1a** with an eclipsed orientation, **1b** in Figure 2, has been also optimized and found to be 21 kJ mol^{-1} higher in energy than **1a**, probably due to the steric hindrance exerted by the CNT π framework. Indeed this value is quite higher with respect to the analogous benzene complexes, where a BE difference of only 1 kJ mol^{-1} between the staggered and the eclipsed conformers was found at the same level of theory.[12b]

A secondary minimum corresponding to a staggered η^2 coordination of the $Cr(CO)_3$ fragment on the C−C bond, **2a** in Figure 2, was found to have a BE of 105 kJ mol^{-1}, i.e. 38 kJ mol^{-1} lower than the BE value of **1a**. The structure **2a** is characterized by an α value of 54° and is computed 41 kJ mol^{-1} lower in energy with respect to the constrained optimized adduct **2a′**, with α = 60°. Rotating the metal fragment by 90° with respect to the C5−C6 bond leads to the structure **2b** shown in Figure 2, that is 30 kJ mol^{-1} higher in energy than the corresponding conformer **2a**.

Furthermore, we found a local minimum structure where the chromium atom is directly bound above a single carbon atom (atop configuration), **3** in Figure 2, with a BE of 68 kJ mol^{-1}, i.e. 75 kJ mol^{-1} higher in energy with respect to the global minimum structure **1a**.

For the sake of completeness, we also performed a full geometry optimization on the $Cr(CO)_3$-(6,0) adduct without any symmetry constraints, setting the metal fragment above the C1−C2 bond (see Scheme 1). The converged structure shows the $Cr(CO)_3$ complex almost on the middle of the ring, analogously to the **1a** configuration discussed above. This confirms that the structure **1a** represents the global minimum of the potential energy surface for the $Cr(CO)_3$-(6,0) adduct and suggests that there is no minimum structure corresponding to an η^2 coordination on the C1−C2 bond.

A summary of the calculated BEs for the investigated complexes is reported in Table 1, whereas the optimized geometrical parameters are in Table 2. According to Table 2, the staggered configuration **1a** shows shorter Cr−C bond distances with the C2 and C3 carbon atoms (2.264 Å) than with the C6 and C5 carbon atoms (2.772 Å), while a Cr−C bond distance of 2.221 Å was found for C1 and C4 atoms. On the other hand, the eclipsed configuration **1b** shows the chromium atom lying on the hexagon axes C1−C4, slightly closer to the C4 atom (Cr−C4 = 2.135 Å with respect to Cr−C1 = 2.305 Å). It is interesting to point out that, while planar aromatic systems, modeling graphene sheets, show the metal atom bound at the center of six-member rings,[12a] CNTs evidence an irregular η^6 coordination of the $Cr(CO)_3$ complex, as pointed out by the value of α = 83°. Indeed, the interaction of the π orbitals of the CO carbonyl group, which crosses the C2−C3 bond, with the π density of the curved carbon surface of CNTs, causes the chromium atom slipping slightly away from the center of the hexagon toward the C2−C3 bond. Notably, a BE of 100 kJ mol^{-1} was calculated at the same level of theory for the planar aromatic system circumcoronene, ($C_{54}H_{18}$),[12a] i.e., 43 kJ mol^{-1} lower than the BE calculated for the **1a** structure. The higher BE computed for the (6,0) tube model is essentially due to increased back-donation from the occupied molecular orbitals

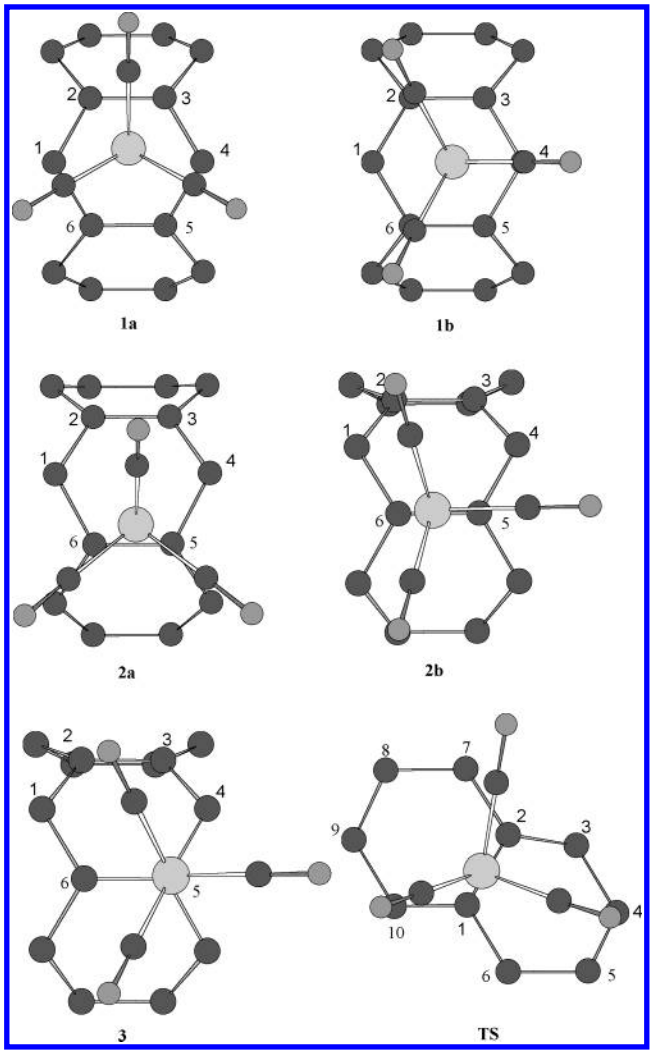

Figure 2. Schematic illustration of the coordination of the $Cr(CO)_3$ fragmentation of the hexagonal ring: the hole site configurations in the staggered **1a** and the eclipsed **1b** orientation, the η^2 configurations **2a** and **2b**, and the atop site configuration **3**. The transition state structure **TS** for the haptotropic migration of the $Cr(CO)_3$ on the CNT sidewalls is also shown.

TABLE 1: Calculated Binding Energies (kJ mol^{-1}) with (BE) and without (BE*) the Correction of the Basis Set Superposition Error (BSSE) for the $Cr(CO)_3$ Complexes with the (6,0)-$C_{72}H_{12}$ Tube Model, According to the Configurations 1−3 Shown in Figure 2

	1a	1b	2a	2b	3
BE*	184	163	144	111	104
BSSE	−41	−41	−39	−36	−36
BE	143	122	105	75	68
DE	15	18	14	13	12
E_{ster}	218	186	140	101	93
E_{orb}	−417	−366	−295	−225	−213
$E_{A'}$	−260	−295	−152	−204	−185
$E_{A''}$	−156	−71	−143	−21	−28

(MO) of the $Cr(CO)_3$ fragment to the empty MOs of the CNT, see below, which is favored by the energy lowering of the empty MOs upon bending the planar aromatic framework.[12a]

The optimized structure for **2a**, with $\alpha = 54°$, shows that the chromium atom does not lie exactly above the C5−C6 bond; instead it is slightly shifted toward the middle of the hexagon, reaching a chromium−carbon bond distance of 2.160 Å for C5 and C6 atoms. Analogously, the **2b** configuration shows the chromium atom closer to the C6 atom (Cr−C6 = 2.193 Å) rather than to the C5 atom (Cr−C5 = 2.339 Å). A different situation is found for the atop site configuration, where the metal atom results essentially bound to the C5 carbon atom in an η^1 bond fashion, with Cr−C5 = 2.097 Å being the shortest Cr−C bond distance among the optimized complexes. The calculated BE values for the $Cr(CO)_3$-(6,0) complexes **1**−**3** are related to the optimized geometrical parameters, showing that a larger hapticity of the chromium atom on the hexagonal ring accomplishes a stronger metal−ligand interaction (see Tables 1 and 2).

TABLE 2: Calculated Cr−C Bond Distances (Å) for the $Cr(CO)_3$ Complexes with the (6,0)-$C_{72}H_{12}$ Tube Model, According to the Configurations 1−3 and the Transition State (TS) Shown in Figure 2

	1a	1b	2a	2b	3	TS
Cr−C1	2.221	2.305	2.643	3.018	2.435	2.177
Cr−C2	2.264	2.544	3.444	4.010	4.150	2.451
Cr−C3	2.264	2.478	3.444	4.098	2.925	3.556
Cr−C4	2.221	2.135	2.643	3.251	2.818	3.918
Cr−C5	2.772	2.478	2.160	2.339	2.097	3.410
Cr−C6	2.772	2.544	2.160	2.193	2.522	2.735

To gain insight into the interaction of $Cr(CO)_3$ fragment with the (6,0) CNT sidewalls, we investigated the electronic structure of the more stable $Cr(CO)_3$-(6,0) adduct **1a** by considering the main MO components of the interaction in the MOs correlation diagram of Figure 3. The analysis of the electronic structure of the $Cr(CO)_3$-(6,0) adduct shows that the interaction is accomplished through electron back-donation to the empty orbitals of the (6,0) tube from the occupied orbitals of the metal with suitable symmetry, and electron donation from the occupied orbitals of the tube with π electron density on the hexagonal ring to the unoccupied orbital of the metal. The highest occupied molecular orbital (HOMO), 90a′, results from electron back-donation of σ type from the occupied orbital of the metal fragment, 11a′ orbital, showing mostly a d_{z^2} character, to the unoccupied MO of the tube, 81a′, with π character on the C1 and C4 atom (see Figure 2 for atom labels). On the other hand, the electron donation from the (6,0) ligand to the metal complex is of π type and involves the occupied MOs of the tube, 70a″ and 71a″, showing π* character on the C1 and C4 carbon atoms, and the 8a″ orbital with d_{xz} character. The contribution of electron σ back-donation is dominant over that of the π donation, as suggested by the decomposition energy scheme reported in Table 1, showing that the energy contribution associated with the A′ representation (−260 kJ mol^{-1}) is much higher than that associated with the A″ representation (−156 kJ mol^{-1}).

3.1. Car—Parrinello Calculations. To gain some insight into the dynamical properties of the $Cr(CO)_3$-(6,0) complex and the haptotropic rearrangement of the metal fragment on the CNT sidewalls, we performed Car−Parrinello simulations using a (6,0)-C_{72} CNT unit periodically repeated. This corresponds to the periodically repeated $C_{72}H_{12}$ model, used for static DFT calculations, without terminal hydrogen atoms. Notably, small differences were found between the geometrical parameters of the $Cr(CO)_3$-(6,0) complex **1b** computed with the ADF and the CP program. In particular the Cr−C bond distances with the C1, C2, C3, and C4 atoms were found equal to 2.300, 2.517, 2.453, and 2.141 Å, respectively, which compare very well with the data reported in Table 2 for the **1b** adduct.

We started the dynamical simulation by heating the structure of the $Cr(CO)_3$ adduct **1b** in its optimized geometry, at a temperature of 500 K. To obtain a thermal distribution of vibrational modes, the temperature was gradually increased, applying a Nosé thermostat[34,35] on both the nuclear and electronic degrees of freedom, thus creating a canonical (*NVT*) ensemble. To allow all the degrees of freedom to evolve

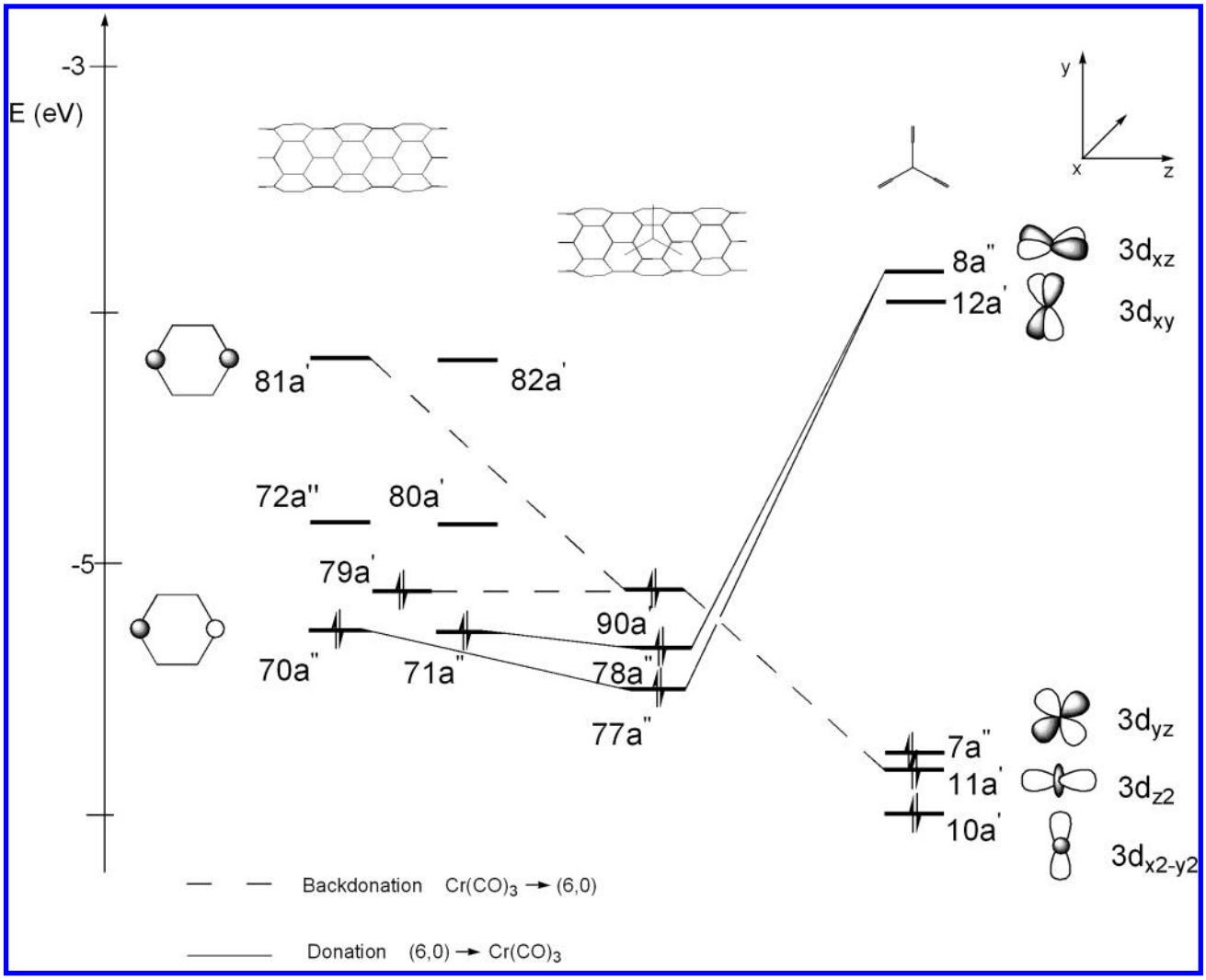

Figure 3. Main MOs components of the interaction for the $Cr(CO)_3$-(6,0)complex in the staggered configuration **1a**.

naturally in time, we did not apply any constraints to the molecular motion; after 2.0 ps of thermalization, the system was observed for a time span of 1.5 ps.

The main result of the dynamical simulation is that the migration of the metal complex occurs between hexagons belonging to two adjacent belts, rather than between hexagons belonging to the same belt, i.e., according to Scheme 1, from one hexagon of belt **A** to one hexagon of belt **B**.

The dynamics of the $Cr(CO)_3$ shifting on the CNT sidewalls can be followed by studying the time evolution of several geometrical parameters of the (6,0)-$Cr(CO)_3$ adduct. In particular, we will analyze the Cr−C4 and Cr−C9 bond distance values as a function of the simulation time, which give at once an estimate of the proceeding of the $Cr(CO)_3$ shifting from belt **A** to **B**. Indeed, the Cr−C4 is expected to grow from ca. 2.2 Å in the initial configuration, to a value larger than 4.0 Å after the haptotropic rearrangement has taken place; on the other hand, a shortening of the Cr−C9 distance is expected as the $Cr(CO)_3$ fragment migrates from belt **A** to **B**. Figure 4 displays the variation of the Cr−C9 and Cr−C4 distances as a function of the simulation time and clearly shows that a haptotropic migration takes place within ca. 2.9 ps. As we can see, a fast increase in the Cr−C4 distance from ca. 2.2 Å, corresponding to a bond length close to the equilibrium value in the initial configuration, to ca. 3.3 Å is observed starting around 2.4 ps; at the same time, the Cr−C9 distance follows an almost complementary trajectory with respect to the Cr−C4 distance, decreasing from an initial value close to 4.5 Å to ca. 3.3 Å within 2.5 ps, reflecting the achievement of a geometrical arrangement characterized by comparable values of the Cr−C4 and Cr−C9 distances. After 2.8 ps, both Cr−C4 and Cr−C9 relax to values close to 2.2 and 4.5 Å, respectively, reflecting the shifting process leading $Cr(CO)_3$ from belt **A** to **B**. A movie file of the CP trajectory is available in the Supporting Information.

To provide a unified picture of the $Cr(CO)_3$ sampling of the CNT sidewalls, we also plotted the time average of the projection of the chromium atom position on the average plane defined by the two hexagons on belts **A** and **B** in Figure 5. The plot in Figure 5 points out that in the investigated time slice the system samples three regions, corresponding to the symmetric hole site minima **1** on belts **A** and **B**, and to an intermediate region located around the C1−C2 bond, which separates the two minima basins and may indicate the transition state (**TS**) region. In particular Figures 4 and 5 suggest that before 2.4 ps the $Cr(CO)_3$ fragment lies almost in the middle of the hexagon ring **A**, in a configuration resembling that of the hole site minima **1**; afterward, in the simulation time slice from 2.4 to 2.8 ps, the shifting process occurs.

Extracting selected configurations from the AIMD run, we were able to optimize the **TS** for the $Cr(CO)_3$ migration, finding a structure 68 kJ mol^{-1} above the global minimum structure **1a**, i.e. 47 kJ mol^{-1} above **1b**. The computed **TS** structure, reported at the bottom of Figure 2, shows the metal fragment

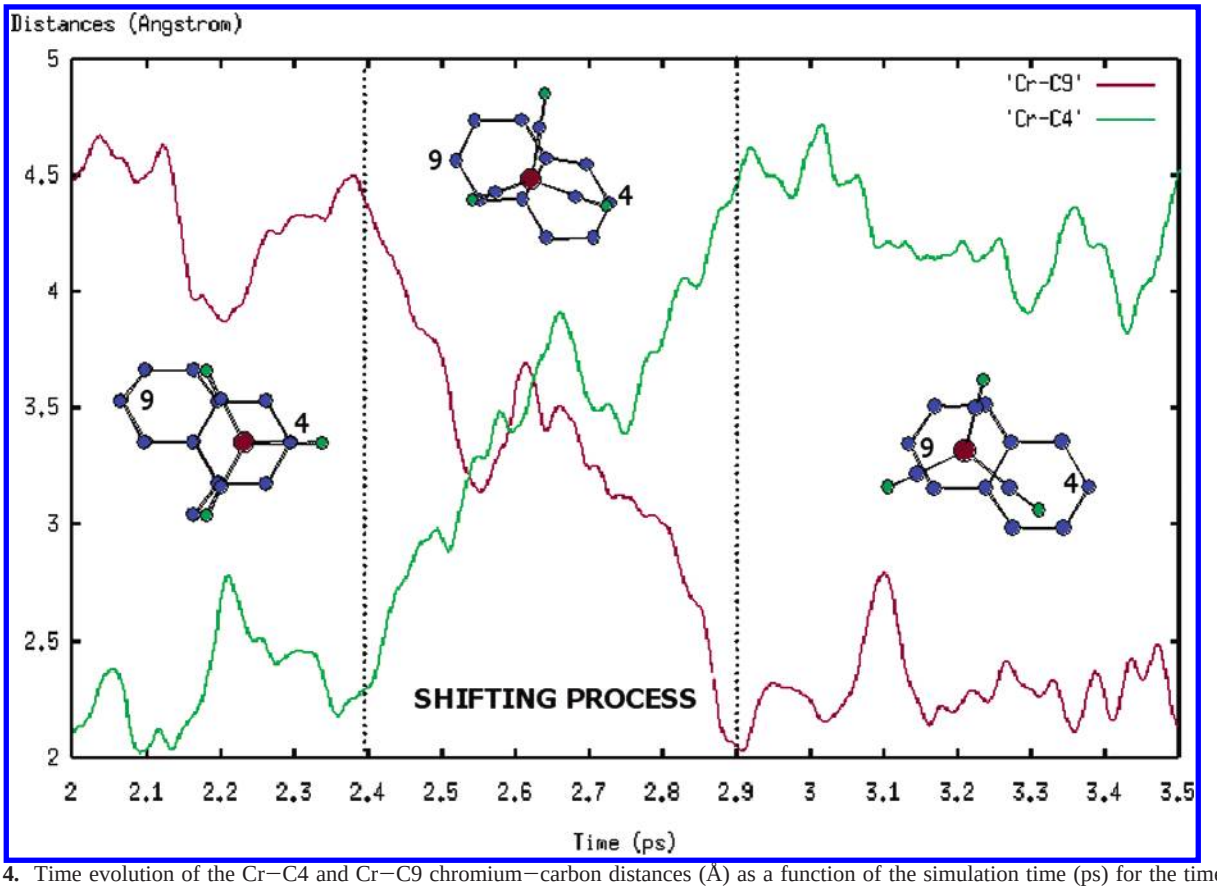

Figure 4. Time evolution of the Cr−C4 and Cr−C9 chromium−carbon distances (Å) as a function of the simulation time (ps) for the time span 2.0−3.5 ps. The left and right regions correspond to the two symmetric hole site minima **1** on belt **A** and **B**, respectively; the central region corresponds to the transition state.

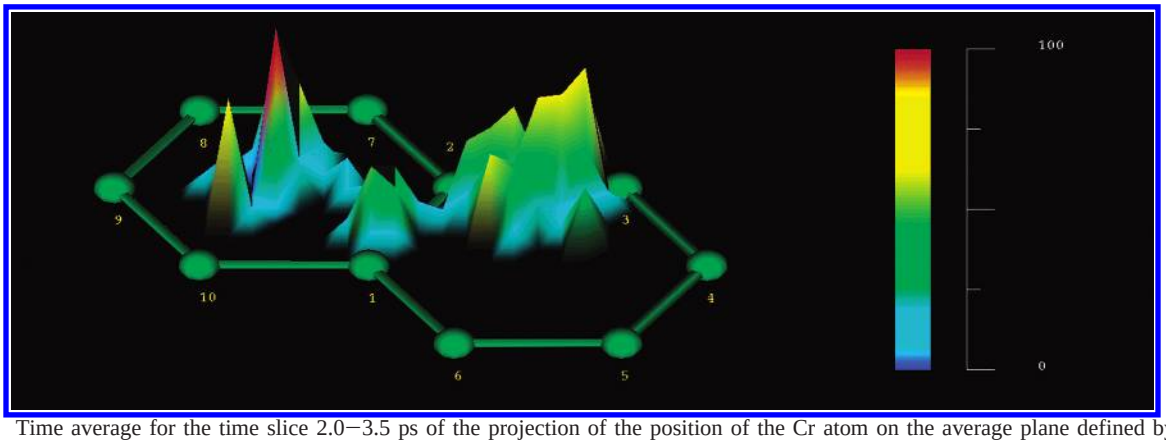

Figure 5. Time average for the time slice 2.0−3.5 ps of the projection of the position of the Cr atom on the average plane defined by the two hexagons belonging to belts **A** and **B**.

across the C1−C2 bond in an η^2 coordination. It is interesting to notice that the computed **TS** structure is not perfectly symmetric with respect to the C1−C2 carbon bond, as suggested by computed Cr−C1 and Cr−C2 bond distances of 2.177 and 2.451 Å, respectively. Notably, Albright and Hoffmann found a potential energy maximum in the middle of the C−C bond connecting adjacent hexagons for the $Cr(CO)_3$ shifting on naphthalene.[16a] It is interesting to note that the **TS** structure described above, related to an η^2 coordination of the $Cr(CO)_3$ on the C1−C2 carbon bond, effectively corresponds to the region located around the C1−C2 bond in Figure 5, connecting the two minima basins.

The picture extracted from the AIMD simulations is consistent with the potential energy surface described by the static calculations, showing that the shifting of the $Cr(CO)_3$ fragment from **A** to **B** hexagons is favored over the shifting within belts **A**. Indeed, crossing of the $Cr(CO)_3$ fragment over the C2−C3 bond would involve passing through structure **2a′**, which is found to be 13 kJ mol^{-1} higher than the computed energy barrier for the shifting along the C1−C2 bond.

In summary, we have shown that a haptotropic migration of the $Cr(CO)_3$ fragment may be accomplished from **A** to **B** hexagons by means of a "bond-following" mechanism, with the metal fragment consecutively slipping above the C3−C2 and C2−C1 bonds (see arrows in Scheme 1), rather than by means of a "bond-crossing" mechanism within hexagons of the same belt, with the metal fragment crossing the C2−C3 bond.

4. Conclusions

In this work, the coordination and the haptotropic rearrangements of the $Cr(CO)_3$ complex on the $(n,0)$ nanotubes sidewalls

has been investigated by means of both static and dynamical density functional theory calculations.

The global minimum structure for the $Cr(CO)_3-(C_{72}H_{12})$ is constituted by a hole site configuration **1a**, where the $Cr(CO)_3$ complex arranges in an irregular η^6 coordination on the hexagonal ring, assuming a staggered orientation with respect to the underlying C−C bonds. A BE of 143 kJ mol^{-1} was computed for this structure. A secondary minimum, **2a**, corresponding to a staggered η^2 coordination of the $Cr(CO)_3$ complex on the C−C bond, was computed with a BE of 105 kJ mol^{-1}, i.e., 38 kJ mol^{-1} higher than the BE calculated for **1a**. Also, a local minimum structure with a BE of 68 kJ mol^{-1} was found with the chromium atom directly bound above a single carbon atom (atop configuration, **3**). The dynamical properties of the $Cr(CO)_3$-(6,0) complex and the haptotropic rearrangement of the metal fragment on the nanotubes sidewalls have been investigated by means of Car−Parrinello simulations, from which a transition state structure for the $Cr(CO)_3$ shifting between two coordination sites on adjacent hexagonal rings was optimized and found to be 68 kJ mol^{-1} above the global minimum structure **1a**.

Further experimental and theoretical efforts are requested in order to rationalize the electronic factors leading to an effective covalent functionalization of carbon nanotubes.

Supporting Information Available: An MPEG movie file showing the CP haptotropic rearrangement trajectory of $Cr(CO)_3$ on the CNT. This material is available free of charge via the Internet at http://pubs.acs.org.

References and Notes

(1) For a review on this topic, see for instance: *Acc. Chem. Res.* **2001**, *34* (6); *Acc. Chem. Res.* **1999**, *32* (5).

(2) Iijima, S. *Nature (London)* **1991**, *354*, 56.

(3) *Acc. Chem. Res.* **2002**, *35* (12). (b) *Carbon Nanotubes: Synthesis, Structure, Properties, and Applications*; Dresselhaus, M. S., Dresselhaus, G., Avouris, Ph., Eds.; Springer-Verlag: Berlin, 2001. (c) Odom, T. W.; Huang, J. L.; Kim, P.; Lieber, C. M. *J. Phys. Chem. B* **2000**, *104*, 2794.

(4) Georgakilas, V.; Kordatos, K.; Prato, M.; Guldi, D. M.; Holzinger, M.; Hirsch, A. *J. Am. Chem. Soc.* **2002**, *124*, 760. (b) Georgakilas, V.; Tagmatarchis, N.; Pantarotto, D.; Bianco, A.; Briand, J.-P.; Prato, M. *Chem. Commun.* **2002**, *124*, 14318. (c) Guldi, D. M.; Marcaccio, M.; Paolucci, D.; Paolucci, F.; Tagmatarchis, N.; Tasis, D.; Vázquez, E.; Prato, M. *Angew. Chem., Int. Ed.* **2003**, *42*, 4206. (d) Sun, Y. P.; Fu, K. F.; Lin, Y.; Huang, W. *Acc. Chem. Res.* **2002**, 35, 1096.

(5) Banerjee, S.; Wong, S. S. *Nano Lett.* **2002**, *2*, 49.

(6) Banerjee, S.; Wong, S. S. *J. Am. Chem. Soc.* **2002**, *124*, 8940.

(7) Fagan, S. B.; da Silva, A. J. R.; Mota, R.; Baierle, R. J.; Fazzio, A. *Phys. Rev. B* **2003**, *67*, 033405. (b) Chiu, P. W.; Duesberg, G. S.; Dettlaff-Weglikowska, U.; Roth, S. *Appl. Phys. Lett.* **2002**, *80*, 3811. (c) Garg, A.; Sinnott, S. B. *Chem. Phys. Lett.* **1998**, *295*, 273. (d) Seifert, G.; Köhler, T.; Frauenheim, T. *Appl. Phys. Lett.* **2000**, *77*, 1313.

(8) For recent reviews on chemical derivatization on carbon CNTs, see for instance: Hirsch, A. *Angew. Chem., Int. Ed.* **2002**, *41*, 1853. (b) Bahar, J. L.; Tour, J. M. *Mater. Chem.* **2002**, *12*, 1952. (c) Niyogi, S.; Hamon, M. A.; Hu, H.; Zhao, B.; Bhowmik, P.; Sen, R.; Itkis, M. E.; Haddon, R. C. *Acc. Chem. Res.* **2002**, *35*, 1105. (c) Banerjee, S.; Kahn, M. G. C.; Wong, S. S. *Chem.—Eur. J.* **2003**, *9*, 1898.

(9) Dagani, R. *Chem. Eng. News* **1999**, *77* (2), 31.

(10) Giannozzi, P.; Car, R.; Scoles, G. *J. Chem. Phys.* **2003**, *118*, 1003. (b) Fagan, S. B.; Mota, R.; da Silva, A. J. R.; Fazzio, A. *Phys. Rev. B* **2003**, *67*, 205414. (c) Yang, C. K.; Zhao, J. J.; Lu, J. P. *Phys. Rev. B* **2002**, *66*, 041403. (d) Andriotis, A. N.; Menon, M.; Froudakis, G. E. *Appl. Phys. Lett.* **2000**, *76*, 3890 and references therein.

(11) Lu, X.; Tian, F.; Xu, X.; Wang, N.; Zhang, Q. *J. Am. Chem. Soc.* **2003**, *125*, 10459 and references therein. (b) Froudakis, G. E. *J. Phys.-Condens. Mater.* **2002**, *14*, R453. (c) Bettinger, H. F.; Kudin, K. N.; Scuseria, G. E. *J. Am. Chem. Soc.* **2001**, *123*, 12849. Kudin, K. N.; Bettinger, H. F.; Scuseria, G. E. *Phys. Rev. B* **2001**, *63*, 45413. (d) Basiuk, V. A.; Basiuk, E. V.; Saniger-Blesa, J. M. *Nano Lett.* **2001**, *1*, 657. (e) Bauschlicher, C. W.; So, C. R. *Nano Lett.* **2002**, *2*, 337 and references therein.

(12) Nunzi, F.; Mercuri, F.; Sgamellotti, A.; Re, N. *Mol. Phys.* **2003**, *101*, 2047. (b) Nunzi, F.; Mercuri, F.; Sgamellotti, A.; Re, N. *J. Phys. Chem. B* **2002**, *106*, 10622.

(13) Lu, X.; Tian, F.; Feng, Y. B.; Xu, X.; Wang, N. Q.; Zhang, Q. N. *Nano Lett.* **2002**, *2*, 1325.

(14) Elian, M.; Chen, M. M.-L.; Mingos, D. M. P.; Hoffmann, R. *Inorg. Chem.* **1976**, *15*, 1148. (b) Muetterties, E. L.; Bleeke, J. R.; Wucherer, E. J.; Albright, T. A. *Chem. Rev.* **1982**, *82*, 499. (c) Bérces, A.; Ziegler, T. *J. Phys. Chem.* **1994**, *98*, 13233.

(15) Suresh, C. H.; Koga, N.; Gadre, S. R. *Organometallics* **2000**, *19*, 3008. (b) Li, J.; Hunter, A. D.; McDonald, R.; Santarsiero, B. D.; Bott, S. G.; Atwood, J. L. *Organometallics* **1992**, *11*, 3050 and references therein.

(16) Albright, T. A.; Hofmann, P.; Hoffmann, R.; Lillya, C. P.; Dobosh, P. A. *J. Am. Chem. Soc.* **1983**, *105*, 3396. (b) Howell, J. A. S.; Ashford, N. F.; Dixon, D. T.; Kola, J. C.; Albright, T.; Kang, S. K. *Organometallics* **1991**, *10*, 1852. (c) Low, A. A.; Hall, M. B. *Int. J. Quantum Chem.* **2000**, *77*, 152. (d) Semmelhack, M. F.; Chlenov, A.; Wu, L.; Ho, D. *J. Am. Chem. Soc.* **2000**, *123*, 8438.

(17) The term "haptotropic" was first introduced by Ahn et al. (Anh, N. T.; Elian, M.; Hoffmann, R. *J. Am. Chem. Soc.* **1978**, *100*, 110) as an extension of "sigmatropic". The latter refers specifically to σ-bond shifts, while the former relates to the more general connotation of changing coordination type.

(18) Car, R.; Parrinello, M. *Phys. Rev. Lett.* **1985**, *55*, 2471.

(19) Baerends, E. J.; Ellis, D. E.; Rosa, P. *Chem. Phys.* **1973**, *2*, 41. (b) Boerrigter, P. M.; Velde, G.; Baerends, E. J. *Int. J. Quantum Chem.* **1998**, *33*, 87.

(20) Vosko, S. H.; Wilk, L.; Nusair, M. *Can. J. Phys.* **1980**, *58*, 1200.

(21) Becke, A. D. *Phys. Rev.* **1988**, *A38*, 2398.

(22) Perdew, J. P. *Phys. Rev.* **1986**, *B33*, 8822.

(23) Ziegler, T.; Rauk, A. *Theor. Chim. Acta* **1977**, *46*, 1. (b) Ziegler, T. *NATO ASI* **1986**, C176, 189.

(24) Boys, S. F.; Bernardi, F. *Mol. Phys.* **1970**, *19*, 553.

(25) Nunzi, F.; Sgamellotti, A.; Re, N. *Organometallics* **2000**, *19*, 1628. (b) Nunzi, F.; Sgamellotti, A.; Re, N.; Floriani, C. *J. Chem. Soc., Dalton Trans.* **1999**, 3487.

(26) Giannozzi, P.; De Angelis, F.; Car, R. *J. Chem. Phys.* **2004**, *120*, 5903.

(27) Pasquarello, A.; Laasonen, K.; Car, r.; Lee, C.; Vanderbilt, D. *Phys. Rev. Lett.* **1992**, *69*, 1982. (b) Pasquarello, A.; Laasonen, K.; Car, R.; Lee, C.; Vanderbilt, D. *Phys. Rev. B* **1993**, *47*, 10142.

(28) Vanderbilt, D. *Phys. Rev. B* **1990**, *41*, 7892.

(29) Perdew, J. P.; Zunger, A. *Phys. Rev. B* **1981**, *23*, 5048.

(30) Perdew, J. P.; Chevary, J. A.; Vosko, S. H.; Jackson, K. A.; Pederson, M. R.; Singh, D. J.; Fiolhais, C. *Phys. Rev. B* **1992**, *46*, 6671.

(31) Fantacci, S.; De Angelis, F.; Sgamellotti, A.; Re, N. *Organometallics* **2001**, *20*, 4031. (b) Fantacci, S.; De Angelis, F.; Sgamellotti, A.; Re, N. *Organometallics* **2002**, *21*, 4090. (c) De Angelis, F.; Fantacci, S.; Sgamellotti, A.; Re, N. *Theor. Chem. Acc.* **2003**, *110*, 196.

(32) Niyogi, S.; Hamon, M. A.; Hu, H.; Zhao, B.; Bhowmik, P.; Sen, R.; Itkis, M. E.; Haddon, R. C. *Acc. Chem. Res.* **2002**, *35*, 1105.

(33) Saito, R.; Dresselhaus, G.; Dresselhaus, M. S. *Physical properties of carbon nanotubes*; Imperial College Press: London, 1998.

(34) Nosé, S. *Mol. Phys.* **1984**, *52*, 255.

(35) Hoover, W. G. *Phys. Rev. A* **1985**, *31*, 1695.